Refractive index inhomogeneity within an aerogel block

T. Bellunato[a], M. Calvi[a], C.F. Da Silva Costa[a,b], C. Matteuzzi[a], M. Musy[a], D.L. Perego[a,c],*

[a]Università degli Studi di Milano—Bicocca and INFN, Milano, Italy
[b]Ecole Polytechnique Fédérale de Lausanne (EPFL), Lausanne, Switzerland
[c]CPPM—Centre de Physique des Particules de Marseille, CNRS/IN2P3, Marseille, France

Abstract

Evaluating local inhomogeneities of the refractive index inside aerogel blocks to be used as Cherenkov radiator is important for a high energy physics experiment where angular resolution is crucial. Two approaches are described and compared. The first one is based on the bending of a laser beam induced by refractive index gradients along directions normal to the unperturbed optical path. The second method exploits the Cherenkov effect itself by shooting an ultra-relativistic collimated electron beam through different points of the aerogel surface. Local refractive index variations result in sizable differences in the Cherenkov photons distribution.
© 2005 Elsevier B.V. All rights reserved.

1. Introduction

Silica aerogel is an amorphous solid network of SiO_2 nanocrystals, with an extremely low macroscopic density. It is transparent and its optical quality is usually defined in terms of two quantities A and C, which parametrize the surface scattering and the bulk Rayleigh scattering of light [1]. Threshold Cherenkov counters based on aerogel exist since decades [2–4]. The use of aerogel as radiator for Ring Imaging Cherenkov (RICH) detectors [5], however, demands extremely good and uniform optical properties [6–8]. Such good quality material has been recently obtained [9], and several experiments have built RICH detectors with aerogel, like HERMES [10], or plan to build one, like LHCb [11–15], AMS [16] and BELLE [17].

In this note we discuss two methods to quantify the inhomogeneity of the refractive index inside an aerogel block. All the measurements have been performed on hygroscopic aerogel tiles produced by the Boreskov Institute of Catalysis in Novosibirsk.

2. Refractive index uniformity

What makes silica aerogel particularly suitable for RICH detectors is that its refractive index n can be chosen in the range 1.008–1.1 [18], since the manufacturer can tune the material density ρ, and n and ρ are related by

$$n(\lambda) = 1 + k(\lambda)\rho, \tag{1}$$

where k is a wavelength-dependent coefficient. Typically, if the density is expressed in g/cm^3, $k = 0.21$ at $\lambda = 400\,nm$. The knowledge of this coefficient is necessary for a fast and simple refractive index control during production.

Local density inhomogeneities lead to point to point variations of the refractive index within the monoliths. These variations contribute to the Cherenkov angle θ_C uncertainty in RICH detectors. For LHCb aerogel, the maximum allowed R.M.S. variation $\sigma(n-1)/(n-1)$ is 1%, corresponding, for $n = 1.030$, to an uncertainty $\sigma(\theta_C) \simeq 1.17\,mrad$.

A method to study possible refractive index inhomogeneities, shown in Fig. 1, uses a laser beam directed

*Corresponding author. Università degli Studi di Milano—Bicocca and INFN, Milano, Italy. Tel.: +39 02 64482507.
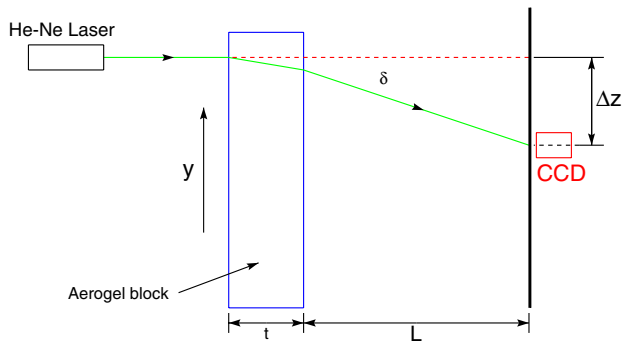E-mail address: Davide.Perego@mib.infn.it (D.L. Perego).
URL: http://castore.mib.infn.it/~dperego.

Fig. 1. Set-up for the laser beam method used to study the refractive index uniformity.
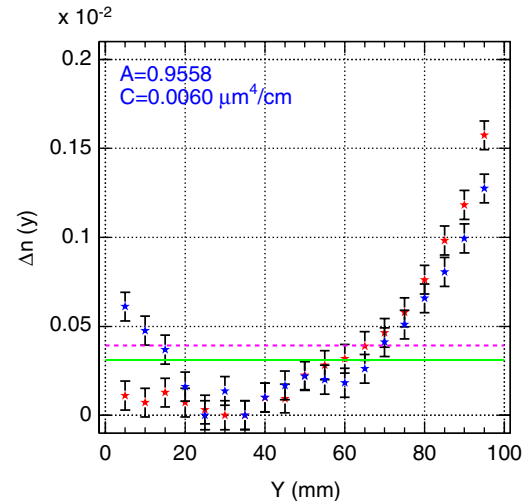

Fig. 2. Result of the scan of a tile with the laser deflection method. The solid line shows the maximum $\sigma(n)$ allowed by the LHCb specifications, the dashed line shows the measured value of $\sigma(n)$, combining the two data series corresponding to different scans along two orthogonal directions on a $100 \times 100 \times 41 \, mm^3$ tile.

perpendicular to the aerogel surface in order to measure deviations from the straight optical path [19,20]. The deviation angle δ is proportional to the refractive index gradient, $dn/dy = n \cdot \delta/t$, where t is the thickness of the block. Scanning $\delta(y)$ along the y direction, the integrated variation can be determined:

$$\Delta n(y) = \frac{n}{t} \cdot \int_{y_0}^{y} \delta(y) \, dy. \qquad (2)$$

We use a CCD camera[1] mounted on a micrometric rail placed at about 2 m from the aerogel exit surface. The displacement of the laser spot is measured with 100 μm resolution. Fig. 2 shows the result of one such measurement. The biggest limitation of this method is that only one wavelength at a time is used, and there is a certain arbitrariness in extrapolating the result to the wavelength range relevant for the Cherenkov emission.

An alternative method was therefore developed, based on the use of a charged particle beam of velocity $\beta = 1$. This method exploits the Cherenkov effect itself, and it is therefore appropriate to study the influence of refractive index variations convoluted with the emission spectrum on the Cherenkov angle reconstruction performance.

The idea underlying this method is that, by letting the beam enter the aerogel surface in different points, any local change in the refractive index reflects in a different distribution of the Cherenkov photons emission angle.

Two table-top Cherenkov counters have been designed and built, under the acronym "APACHE" for *Aerogel Photographic Analysis by CHerenkov Emission*, with photographic film as photodetectors. The first one, which was rather a feasibility test, consisted in a simple proximity focused Cherenkov detector. It was very useful to get a quick feedback on the potential of the method, but the resolution was too poor for our purposes. In this configuration, in fact, the thickness of the detected Cherenkov ring is directly proportional to the aerogel thickness. This problem was overcome with the introduction of a focusing spherical mirror in the design; the second

and final set-up was then a proper RICH detector and it will be described in the next section.

3. APACHE

A light tight anodized aluminium vessel provides the housing for all the components of APACHE. The set-up has been installed at the 500 MeV electron beam of the DAΦNE Beam Test Facility in Frascati (BTF) [21]. The electron beam, producing saturated Cherenkov rings in the aerogel, is used to scan the index of refraction varying the entrance point of the beam in the aerogel block. Black & white $8'' \times 10''$ photographic films[2] have been used as photodetectors. Due to the relatively poor detection efficiency of the film, a rather high integrated fluence was needed in order to have a neat image. On average, 350 bunches of about 3×10^7 electrons were shot on the aerogel for each run. The films have been then processed by a professional photographic laboratory, scanned and digitized for data analysis. The first measurement was taken on a hygroscopic sample $100 \times 100 \times 41 \, mm^3$ in size. The same tile had previously been measured with the laser scan method, Fig. 2, for a cross-check of the results.

A sketch of the set-up is shown in Fig. 3. The aerogel tile is placed on a variable-height platform with the wide faces perpendicular to the beam axis. The volume is flushed with nitrogen to avoid as much as possible a variation of the optical properties of the aerogel due to the absorption of humidity [15]. A spherical mirror with a radius of curvature $R = 949 \, mm$ is placed downstream of the aerogel, vertically tilted with respect to the beam line. The vertical tilt

---

[1]SONY® XC–ST70CE with 768×512 pixels and sensitive area coverage of $1.025 \times 0.850 \, cm^2$.

[2]Kodak® Professional TRI–X 400 Film/400TX and ILFORD® HP5 Plus 400.
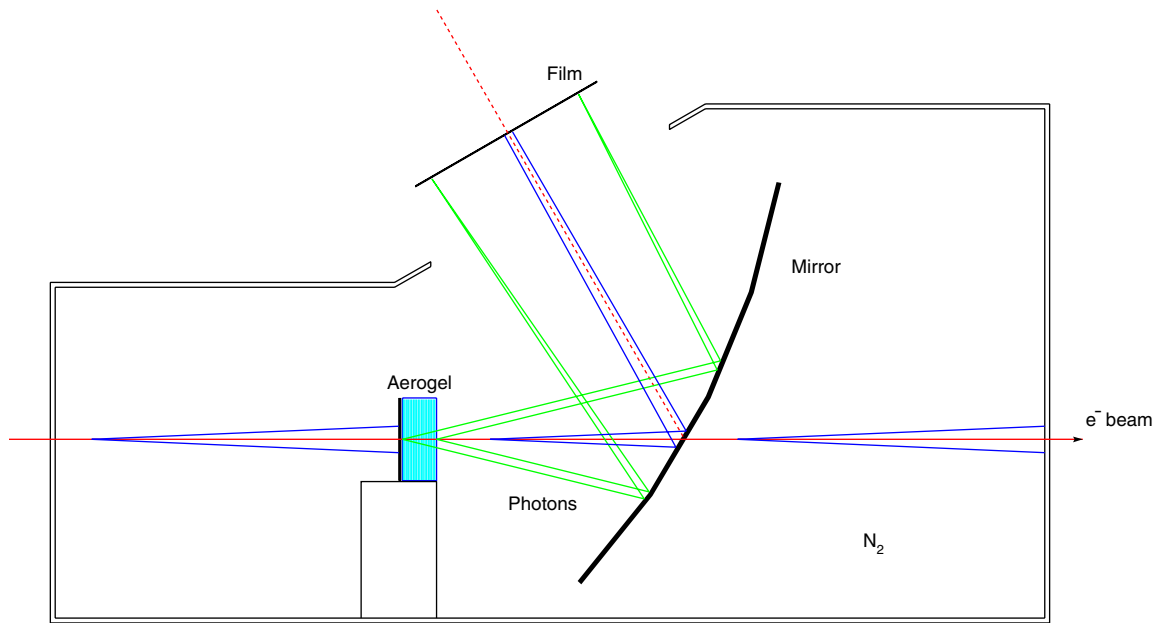
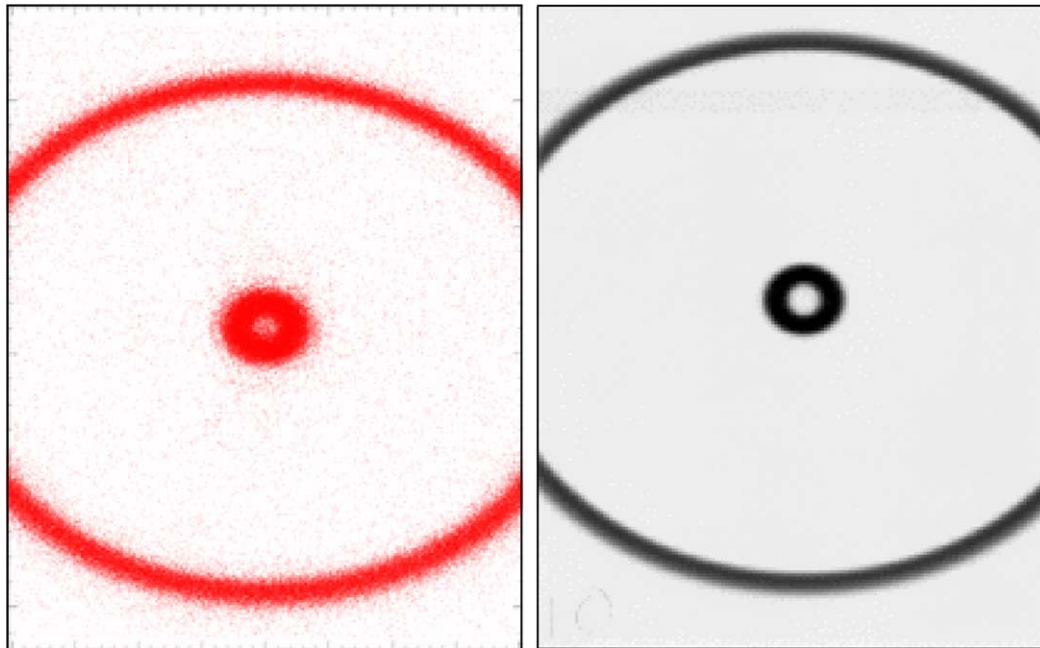Fig. 3. A schematic view of the set-up built for the APACHE runs.

Fig. 4. On the left, GEANT4 simulation of the photon distribution on the film for an APACHE run. On the right, the scanned image of a data film. Part of the aerogel ring fell outside the acceptance due to the limited size of the films.

allows to move the focal surface of the mirror, where the film must be placed in order to collect the focused Cherenkov photons, safely out of the electron beam path.

Rayleigh scattering, whose cross sections scales as λ^{-4}, is the dominant contribution to the total diffusion probability inside aerogel. After a few preliminary runs, data have always been taken with a UV filter[3] between the aerogel and the mirror, in order to kill the most energetic

photons, which have the highest scattering probability. A black paper screen is used to stop the photons produced in nitrogen upstream of the aerogel.

The GEANT4 [22] simulation toolkit has been used to study the systematics involved in data processing and analysis. Apart from the refractive index, many parameters influence the light distribution on the film, such as the direction of the electrons, the scattering probability, the aerogel thickness, the mirror reflectivity and tilt, and the detection efficiency of the film. All the details of the

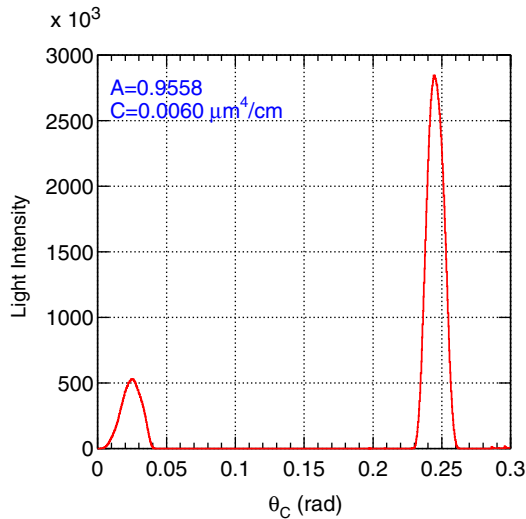[3]D 263 T borosilicate glass by SCHOTT Guinchard SA.

Fig. 5. The Cherenkov angle distribution for an APACHE run. The two peaks refer to photons emitted in nitrogen (low angles) and in aerogel (large angles). The light intensity is expressed in terms of the 8-bit value of the scan.
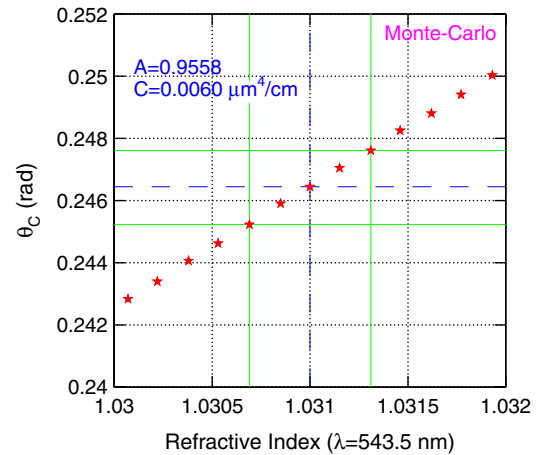

Fig. 6. Displacement of the reconstructed Cherenkov angle peak position for refractive index variations in steps of 0.5%. The dashed lines correspond to the nominal n and θ_C, the solid lines are the $\pm 1\%$ region.

APACHE configuration have been implemented in a dedicated complete simulation.

Fig. 4 is an example of a simulated run and a scanned image of a film of an actual APACHE run. Two rings are clearly seen in both simulation and data. The large ring contains the Cherenkov photons emitted inside the aerogel; the small one is built up by Cherenkov photons emitted in nitrogen between the aerogel and the mirror. The rings are not circular because of the mirror tilt, which introduces non trivial distortions, giving the Cherenkov photons distribution on the film an ellipsoidal shape.

Data analysis has been performed on the digitized images. To limit possible distortions of the Cherenkov light distribution induced by the film processing, a background value is evaluated, taken as the average light intensity in a small film portion close to the side and blinded by the thick opaque holding frame.

From the actual position in space of a photon hit, one can infer its Cherenkov emission angle. The information needed are the versor of the electron beam, the photon emission point, the position in space of the centre of curvature of the mirror and its radius.

The beam direction has been extracted from data. The barycentre of the nitrogen Cherenkov ring has been retracked considering it as the hit point of a photon in the same fashion as for the actual Cherenkov photons, assuming a beam direction along the reference line in the experimental hall. The direction calculated by the retracking procedure has then been taken as the real beam versor for the analysis of the films. An average 24 mrad deviation from the reference line has been measured and corrected for.

A hit by hit retracking algorithm [23] allows to build the distribution of the reconstructed Cherenkov emission angle.

An example of such a distribution is plotted in Fig. 5. From these plots the average shift of the mean reconstructed Cherenkov angle from film to film is extracted, and therefore the point to point variation of n within the aerogel tile. The parameter which best suits for comparison among runs is the angle for which the distribution of Cherenkov photons from aerogel has a maximum.

The analysis of simulated data shows, Fig. 6, the link between a refractive index change and the corresponding shift in the reconstructed Cherenkov angle peak. The simulation requires the value of the refractive index at a certain wavelength: the dispersion curve is then calculated from the aerogel Sellmeier coefficients. The chosen wavelength is $\lambda = 543.5$ nm, that is the λ of the laser we use for measuring the refractive index in the lab. The plot in Fig. 6 has the value of $n(\lambda = 543.5$ nm$)$ on the abscissa, but the full dispersion curve is calculated and used each time.

To study the uncertainties associated with this method the simulation program was run in order to estimate the effect of small changes in the set-up geometry or beam conditions. The beam direction has been varied both as parallel displacement and as a tilt with respect to the nominal beam axis. The film position in space has been varied in order to check the effect of systematic shifts in the reconstruction parameters in the analysis. Since the aim of the experiment is a scan of relative variations of n, it has been proven that small misalignments do not contribute substantially to our accuracy, as long as the conditions are stable from run to run. To check the stability of the conditions, a good indicator is the Cherenkov angle distribution for photons produced in the nitrogen volume between the aerogel and the mirror. The value of the angle for which the nitrogen ring has a maximum is independent of the aerogel, and it is expected to be constant from run to run, apart for tiny refractive index variations due to temperature and pressure changes. Any significant displacement of the nitrogen Cherenkov peak is then to be

Table 1
List of systematic contributions to the angular peak resolution in APACHE

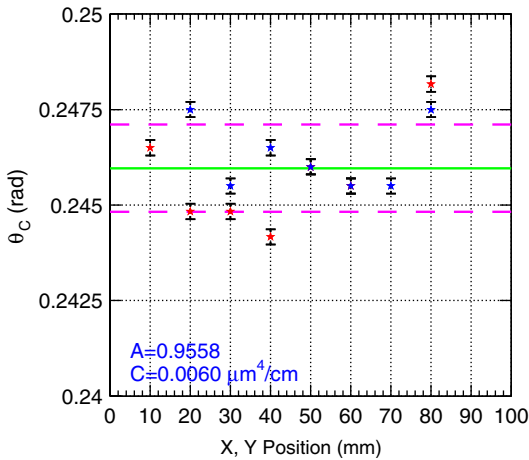| Source	Contribution (mrad)
Beam divergence	0.1
Beam shift	0.1
Beam tilt	0.2
Film position	0.2
Total resolution	0.3

Fig. 7. Summary plot of the results of all APACHE measurements on the aerogel tile. Blue and red data point belong to the horizontal and vertical scans, respectively. The green solid line is the mean value of the average Cherenkov angle for each film. The purple dashed lines give the one-sigma region around the mean value: $\sigma(\theta_C) = 1.14$ mrad.

ascribed to uncontrolled variations of the run conditions. It has been verified on a large set of simulated data, that the precision in the peak position is 0.3 mrad. The contributions to the systematic uncertainties are listed in Table 1.

The scan performed on the aerogel block consisted in 15 points distributed on the surface at which the beam was shot. The variance $\sigma(\theta_C)$ of the angular peak positions in all the films is $\sigma(\theta_C) = 1.14$ mrad and it is shown in Fig. 7. This means that this specific tile complies with the requested specification $\sigma(\theta_C) \leqslant 1.17$ mrad.

3.1. LHCb aerogel

Recently, the first batch of aerogel bricks complying with the LHCb requests on large thickness and transverse dimensions has been produced and delivered. We have tested one of the four tiles, which we will refer to as sample 985–3, at the BTF. The size of the sample is $200 \times 200 \times 50$ mm^3, with Hunt parameters $A = 0.98$ and clarity coefficient $C = 0.0058 \, \mu m^4/cm$. A scan across the surface has been accomplished, 25 points in total. The analysis is the same as the one described in the previous section.
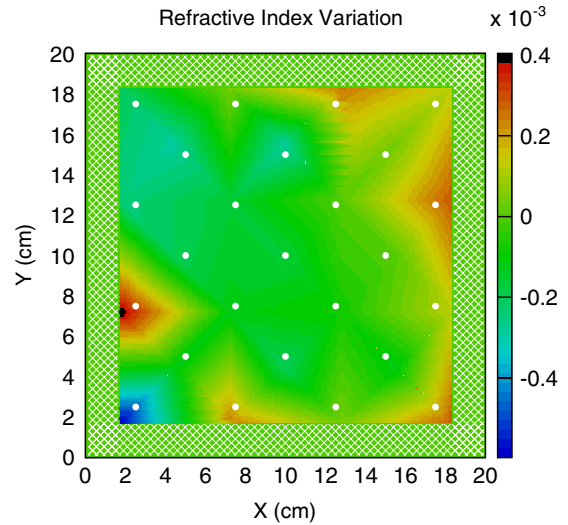

Fig. 8. An interpolated colour map showing the measured deviation from the average Cherenkov angle for each beam entrance point, represented as a white dot.

A summary of these measurements is shown in Fig. 8, where the deviation of the mean Cherenkov angle measured at each run with respect to the average of all measurements is plotted as a function of the coordinates of the beam entrance point on the aerogel surface. The interpolated colour map stops 2 cm from the sides, since no data have been taken with the beam nominal entrance point in that region. The plot suggests a refractive index gradient from the centre of the tile towards the sides, particularly marked on the right hand side. This is understood in terms of the average 24 mrad horizontal deviation of the beam path with respect to the theoretical direction. Since the aerogel is placed at a distance of about 60 cm from the end of the beam vacuum pipe, this means that on average the runs taken on the right hand side of the block have in fact traversed the surface only 6 mm from the aerogel side. Taking into account the beam dimensions $\sigma_x \simeq \sigma_y \simeq 5$ mm we are confident that our scan was complete. We conclude that the mean deviation from the average value of the Cherenkov angle is 0.9 mrad, corresponding to a variation of n within the tile $\sigma(n-1)/(n-1) = 0.76\%$, well within the specifications of our application.

4. Conclusions

A novel technique folding the refractive index spread with the Cherenkov emission spectrum and the detection efficiency of Cherenkov photons, giving directly the weighed average of the Cherenkov angle additional uncertainty has been developed to evaluate the refractive index homogeneity within a silica aerogel tile. A comparison between a purely optical method based on laser beam deflection shows that APACHE is a more effective way of describing the variation of the refractive index gradients inside a tile.

Two aerogel samples of large size and with optical properties matching the strict requirements of the LHCb RICH detector have been tested: one, with dimensions $100 \times 100 \times 41\,mm^3$, was produced in 2003 and just meets the $\sigma(n-1)/(n-1) = 1\%$ specifications. The second tested tile is a $200 \times 200 \times 50\,mm^3$ recently produced for the LHCb RICH detector. The measured refractive index spread in this sample, $\sigma(n-1)/(n-1) = 0.76\%$, is well within the specifications and justifies the confidence that the full aerogel radiator for LHCb can be assembled out of a small number of large size tiles, thus limiting the loss of photons at the interfaces between adjacent tiles.

Acknowledgements

References

[1] A.J. Hunt, et al., Mat. Res. Soc. Symp. Proc. (1984) 275.
[2] M. Cantin, et al., Nucl. Instr. and Meth. A118 (1974) 177.
[3] A.F. Danilyuk, et al., Nucl. Instr. and Meth. A433 (1999) 406.
[4] H. Yokogawa, M. Yokoyama, J. Non-Cryst. Solids 186 (1995) 23.
[5] R. De Leo, et al., Nucl. Instr. and Meth. A401 (1997) 187.
[6] A.K. Gougas, et al., Nucl. Instr. and Meth. A421 (1999) 249.
[7] A.R. Buzykaev, et al., Nucl. Instr. and Meth. A433 (1999) 396.
[8] R. De Leo, et al., Nucl. Instr. and Meth. A457 (2001) 52.
[9] M.Y. Barnykov, et al., Nucl. Instr. and Meth. A419 (1998) 584.
[10] HERMES Collaboration, Nucl. Instr. and Meth. A417 (1998) 230.
[11] LHCb Collaboration, LHCb RICH TDR, CERN/LHCC/2000-0037.
[12] M. Alemi, et al., Nucl. Instr. and Meth. A478 (2002) 348.
[13] T. Bellunato, et al., Nucl. and Instr. Meth. A502 (2003) 227.
[14] T. Bellunato, et al., Nucl. and Instr. Meth. A519 (2004) 493.
[15] T. Bellunato, et al., Nucl. Instr. and Meth. A527 (2004) 319.
[16] R. Battiston, et al., Nucl. Instr. and Meth. A409 (1998) 458.
[17] T. Matsumoto, et al., Nucl. Instr. and Meth. A521 (2004) 367.
[18] A.R. Buzykaev, et al., Nucl. Instr. and Meth. A379 (1996) 465.
[19] L.W. Hrubesh, C.T. Alviso, Mater. Res. Soc. Symp. Proc. 121 (1988) 703.
[20] A.R. Buzykaev, et al., Nucl. Instr. and Meth. A433 (1999) 396.
[21] G. Mazzitelli, et al., Nucl. Instr. and Meth. A515 (2003) 524.
[22] S. Agostinelli, et al., Nucl. Instr. and Meth. A506 (2003) 250.
[23] R. Forty, et al., Nucl. Instr. and Meth. A384 (1996) 167.